Microwave Spectra of Dimethylether $(CH_3)_2O$ and $(CD_3)_2O$ in Excited Torsional States

H. Lutz * and H. Dreizler

Abt. Chemische Physik im Institut für Physikalische Chemie der Universität Kiel

Z. Naturforsch. **33a**, 1498–1510 (1978); received October 11, 1978

Dedicated to Yonezo Morino

The rotational spectra of the torsional excited states $\tilde{v}_n = 1_1, 1_2, 2_1, 2_2, 2_3$ have been measured and assigned. The torsional fine structure was used to determine the coefficients V_3 and V'_{12} of the hindering potential.

For $(CH_3)_2O$: $V_3 = 2618 \pm 4$ cal/mole, $V'_{12} = 18 \pm 8$ cal/mole, for $(CD_3)_2O$: $V_3 = 2572 \pm 6$ cal/mole, $V'_{12} = 29 \pm 12$ cal/mole, V_{12} was correlated to V_3.

Introduction

Dimethylether was one of the first molecules [1] with two methyl tops (two top molecule) investigated by microwave spectroscopy for the determination of the barrier to internal rotation. Usually the hindering potential is described by a two dimensional Fourier series in the torsional angles α_i, $i = 1, 2$. For molecules with two equivalent tops and C_{2v}-symmetry it may be given in the form:

$$V(\alpha_1, \alpha_2) = \frac{V_3}{2}(1 - \cos 3\alpha_1) + \frac{V_3}{2}(1 - \cos 3\alpha_2) + V'_{12} \sin 3\alpha_1 \sin 3\alpha_2 + V_{12} \cos 3\alpha_1 \cos 3\alpha_2 + \cdots . \quad (1)$$

V_3 is the hindering potential, V'_{12} and V_{12} are top-top coupling parameters. The analysis of the rotational spectra is based on a rigid frame rigid top Hamiltonian, which was discussed in detail elsewhere [2–8] and is given later under Equation (2).

This Hamiltonian allows for two internal degrees of freedom, the methyltorsions, and three degrees of freedom for the overall rotation. All other vibrational degrees of freedom are excluded.

By the analysis of the rotational spectrum in the ground-state, V_3 was determined [1, 9]. As in similar cases [10, 11] the top-top coupling coefficient V'_{12} can only be determined, if the rotational spectra of the excited torsional states $\tilde{v}_n = 1_1$ and 1_2** are analysed. For Dimethylether this was done independently by [12–14]. V_{12} could not be determined, as it was correlated to V_3 as noticed in similar work [11]. This correlation may be seen, if the harmonic approximation is calculated.

$$V(\alpha_1, \alpha_2) \approx \frac{9}{4}(V_3 - 2V_{12})(\alpha_1^2 + \alpha_2^2) + 9V'_{12}\alpha_1\alpha_2 . \quad (1a)$$

V_3 and V_{12} are combined in the coefficient of $\alpha_1^2 + \alpha_2^2$. Our investigation presented in this paper was initiated to determine the top-top coupling coefficient V_{12} [see Eq. (1)] from the rotational spectra of the torsional excited states $\tilde{v}_n = 2_1, 2_2, 2_3$, as a consideration of the Hamiltonian showed that at least these spectra should be included in the analysis. As the 2_n-states are near to half the barrier height V_3, we believed, that (1a) is no more a good approximation. But it proved finally, that V_{12} is still correlated to V_3. Nevertheless we like to give the results as to our knowledge a detailed analysis of rotational spectra of the torsional excited states $\tilde{v}_n = 2_1, 2_2, 2_3$ for a two top molecule is not yet published. Our analysis is applied to the two isotopic forms $(CH_3)_2O$ and $(CD_3)_2O$.

Experimental

The spectra of $(CH_3)_2O$ and $(CD_3)_2O$ were recorded in the region from 8 to 40 GHz by a conventional Stark spectrometer [15, 16] equiped with an 8 m absorption cell and employing 33 kHz Stark square wave modulation. The sample pressure was 10 mT and the temperature was kept between 0 °C and −50 °C. For the assignment of the lines in the higher torsional states microwave-microwave double resonance (MW-MW-DR) experiments proved very useful. The MW-MW-DR-Spectrometer is described in detail in [17]. $(CD_3)_2O$ was supplied by Isocommerz GmbH Leipzig.

* Part of the Ph.D. Thesis of H. Lutz, Kiel 1978.

** For the labelling of the levels see [11].

Reprint requests to Prof. Dr. H. Dreizler, Abt. Chemische Physik, Institut für Physikalische Chemie der Universität Kiel, Olshausenstr. 40–60, D-2300 Kiel.

Measurement and Assignment of the Spectra *

For the assignment of the spectra we used the following criteria:

a) Stark effect;
b) Relative spin weights [6, 7];
c) Boltzmann factors of the different states;
d) Fit of the A_iA_j- and A_iE-rotational lines to a rigid rotor spectrum;
e) Similarities of the frequency shifts with respect to the ground state of the Q-series $J_{0J} - J_{1,J-1}$, $\tilde{v}_n$ for $(CD_3)_2O$ and $(CH_3)_2O$;
f) Double resonances;
g) Theoretical predictions of the internal rotation splittings.

As especially the assignment of the rotational spectra in the 2_n-torsional states was difficult, the combination of all the mentioned criteria was necessary.

As the internal rotation splittings are smaller for $(CD_3)_2O$ we tried to assign this isotopic species first **. The unsplit ground state, $\tilde{v}_n = 0_1$-spectrum had been assigned earlier [19]. The reported lines were measured with higher precission. These and some additionally measured lines are given in Table 1. The lines up to $J = 3$ were fitted by a rigid rotor spectrum. The rotational constants are given in Table 4.

The low J-lines of the states $\tilde{v}_n = 1_1$ and 1_2 were found within a frequency region of ± 300 MHz of the respective ground state lines. They were assigned by the mentioned criteria a)—d). The low J-lines of the states $\tilde{v}_n = 2_1$, 2_2 and 2_3 were located in a ± 400 MHz region. The assignment was possible by application of the criteria a)—d) and g). The measured lines are given in Tables 2 and 3. Table 4 summarises the effictive A_iA_j- and A_iE-rotational constants.

Figures 1 and 2 illustrate the frequency shifts with respect to the ground state lines of the $J_{0,J} - J_{1,J-1}$, $\tilde{v}_n$-series. The regularity within one series is an additional indication for the validity of the assignment.

For $(CH_3)_2O$ the ground state spectrum had been assigned earlier [1, 19]. Additional measurements for astrophysical reasons were made recently [20].

The assignment of the rotational lines of the torsional states $\tilde{v}_n = 1_1$ and 1_2 was successfull first for the $J_{0,J} - J_{1,J-1}$, 1_n-series by the criterion e), which is illustrated in Fig. 1, in combination with criteria a), b) and g). The assignment of an additional $\Delta J = 1$-line for each 1_n-state concluded the assignment. The consistancy was checked with criterion d).

For the 2_n-state spectra the assignment proved to be rather difficult, as the lines are weak and the torsional multipletts are split by about 1 GHz. As a consequence of the large splittings the three 2_n-multipletts are mixed in their order.

The criteria b) and c) cannot be applied as the intensity cannot be determined reliably with our spectrometer for largely splitted multiplets, as the microwave power fluctuates with frequency.

The assignment was guided by the hints given by the similarities of the $(CD_3)_2O$- and $(CH_3)_2O$-spectra [criterion e)] as illustrated in Figure 2. By using the Stark-effect the A_iA_j-components of the $J_{0,J} - J_{1,J-1}$, 2_n-series could be assigned. The EE-components were identified by the Stark-effect, which contains linear contributions, and by application of criterion g) with data gained by the analysis of the 1_n-state spectra. Criterion g) and a)

* For the group theoretical labelling see [6], [7].

** For more details see Ref. [18].

Table 1. Rotational lines of $(CD_3)_2O$ for the $\tilde{v}_n = 0_1$ torsional state [MHz].

$J_{K_-K_+} - J'_{K_-'K_+'}$	ν_{exp}	$J_{K_-K_+} - J'_{K_-'K_+'}$	ν_{exp}	$J_{K_-K_+} - J'_{K_-'K_+'}$	ν_{exp}
$0_{00} - 1_{11}$	32494.43[a]	$4_{04} - 4_{13}$	22216.85[a]	$6_{24} - 7_{17}$	33036.44
$1_{01} - 1_{10}$	18898.26[a]	$4_{23} - 5_{14}$	20761.65	$7_{07} - 7_{16}$	29911.81
$1_{11} - 2_{02}$	10332.22[a]	$5_{24} - 4_{31}$	21473.52	$7_{35} - 8_{26}$	24418.83
$2_{02} - 2_{11}$	19603.00[a]	$4_{22} - 5_{15}$	10201.72	$7_{34} - 8_{27}$	20538.52
$2_{12} - 3_{03}$	25223.63[a]	$5_{23} - 4_{32}$	20811.53	$12_{58} - 13_{49}$	19721.10
$3_{12} - 2_{21}$	10774.87	$5_{05} - 5_{14}$	24219.84[a]	$12_{57} - 13_{4,10}$	19607.15
$3_{13} - 2_{20}$	14907.89	$5_{23} - 6_{16}$	21948.94		
$3_{03} - 3_{12}$	20695.42[a]	$5_{24} - 6_{15}$	36979.37		

[a] Measured by Blukis et al. [19].

Table 2. Rotational lines of $(CD_3)_2O$ for the $\tilde{v}_n = 1_1$ and 1_2 torsional states [MHz].

$J_{K_-K_+} - J'_{K_-'K_+'}$	$\tilde{v}_n$ $\Gamma\Gamma'$	ν_{exp}	$\Delta\nu_{exp}$	$\Delta\nu_{cal}$	$\Delta\nu_{exp} - \Delta\nu_{cal}$	$J_{K_-K_+} - J'_{K_-'K_+'}$	$\tilde{v}_n$ $\Gamma\Gamma'$	ν_{exp}	$\Delta\nu_{exp}$	$\Delta\nu_{cal}$	$\Delta\nu_{exp} - \Delta\nu_{cal}$
$0_{00} \rightarrow 1_{11}$	1_1 A_1A_2	32487.62				$3_{12} - 2_{21}$	1_1 A_1A_2	10936.10			
	EE	32487.88	0.25	0.25	0.00		EE	10936.70	0.60	0.65	-0.05
	A_1E	32488.13	0.51	0.46	0.05		A_1E	10937.35	1.25	1.23	0.02
	EA_2			0.47	0.04		EA_2	10937.25	1.15	1.28	-0.13
	1_2 A_2A_1	32468.75					1_2 A_2A_1	10978.92			
	EE	32468.99	0.24	0.22	0.02		EE	10979.48	0.56	0.56	0.00
	A_2E	32469.23	0.48	0.38	0.10		A_2E	10980.00	1.17	1.03	0.14
	EA_1			0.40	0.08		EA_1	10980.09	1.08	0.96	0.12
$1_{01} \rightarrow 1_{10}$	1_1 A_1A_2	18916.15				$4_{04} - 4_{13}$	1_1 A_1A_2	22211.34			
	EE	18916.41	0.27	0.25	0.02		EE	22211.62	0.29	0.30	-0.01
	A_1E	18916.66	0.51	0.46	0.05		A_1E	22211.91	0.57	0.55	0.02
	EA_2			0.47	0.04		EA_2			0.57	0.00
	1_2 A_2A_1	18881.13					1_2 A_2A_1	22041.16			
	EE	18881.40	0.25	0.22	0.03		EE	22041.43	0.27	0.25	0.02
	A_2E	18881.64	0.51	0.38	0.13		A_2E	22041.69	0.54	0.45	0.09
	EA_1			0.40	0.11		EA_1			0.47	0.07
$1_{11} \rightarrow 2_{02}$	1_1 A_1A_2	10251.78				$4_{23} - 5_{14}$	1_1 A_1A_2	20523.60			
	EE	10251.55	-0.23	-0.22	-0.01		EE	20523.03	-0.57	-0.59	0.02
	A_1E	10251.33	-0.45	-0.41	-0.04		A_1E	20522.46	-1.14	-1.12	-0.02
	EA_2			-0.42	-0.03		EA_2			-1.16	0.02
	1_2 A_2A_1	10241.59					1_2 A_2A_1	20350.59			
	EE	10241.40	-0.19	-0.19	0.00		EE	20350.06	-0.53	-0.54	0.01
	A_1E	10241.19	-0.40	-0.34	-0.06		A_2E	20349.53	-1.06	-0.94	-0.12
	EA_2			-0.36	-0.04		EA_1				
$2_{02} - 2_{11}$	1_1 A_1A_2	19616.14				$5_{23} - 6_{16}$	1_1 A_1A_2	21772.55			
	EE	19616.40	0.26	0.26	0.00		EE	21771.85	-0.69	-0.79	0.10
	A_1E	19616.67	0.53	0.48	0.05		A_1E	21771.16	-1.39	-1.46	0.07
	EA_2			0.49	0.04		EA_2			-1.52	0.13
	1_2 A_2A_1	19553.49					1_2 A_2A_1	22116.45			
	EE	19553.74	0.25	0.22	0.03		EE	22115.80	-0.65	-0.68	0.03
	A_2E	19553.74	0.50	0.39	0.11		A_2E	22115.15	-1.29	-1.20	-0.09
	EA_1			0.42	0.08		EA_1			-1.27	-0.02
$3_{03} - 3_{12}$	1_1 A_1A_2	20700.95				$5_{05} - 5_{14}$	1_1 A_1A_2	24199.16			
	EE	20701.22	0.27	0.27	0.00		EE	24199.47	0.31	0.33	-0.02
	A_1E	20701.49	0.55	0.51	0.04		A_1E	24199.77	0.61	0.61	0.00
	EA_2			0.53	0.02		EA_2			0.63	-0.02
	1_2 A_2A_1	20594.22					1_2 A_2A_1	23942.48			
	EE	20594.48	0.26	0.24	0.02		EE	23942.76	0.28	0.27	0.01
	A_2E	20594.74	0.51	0.42	0.09		A_2E	23943.05	0.56	0.49	0.07
	EA_1			0.44	0.07		EA_1			0.51	0.05
$3_{13} - 2_{20}$	1_1 A_1A_2	15042.03				$4_{22} - 5_{15}$	1_1 A_1A_2	10034.51			
	EE	15042.75	0.72	0.73	-0.01		EE	10033.82	-0.69	-0.76	0.07
	A_1E	15043.48	1.45	1.36	0.09		A_1E	10033.13	-1.38	-1.41	0.03
	EA_2			1.40	0.05		EA_2			-1.46	0.08
	1_2 A_2A_1	-					1_2 A_2A_1	10275.29			
	EE	-		0.67			EE	10274.66	-0.63	-0.66	0.03
	A_2E	-		1.12			A_2E	10274.03	-1.26	-1.16	-0.10
	EA_1	-		1.31			EA_1			-1.24	-0.02
$2_{12} - 3_{03}$	1_1 A_1A_2	25110.64				$5_{24} - 4_{31}$	1_1 A_1A_2	21718.98			
	EE	25110.40	-0.24	-0.20	-0.04		EE	21720.11	1.13	1.23	-0.10
	A_1E	25110.19	-0.45	-0.31	-0.14		A_1E	21720.65	1.67	2.25	-0.58
	EA_2			-0.38	-0.07		EA_2	21721.56	2.58	2.30	0.28
	1_2 A_2A_1	25069.61					1_2 A_2A_1	21652.63			
	EE	25069.40	-0.20	-0.18	-0.02		EE	21653.71	1.09	1.50	-0.41
	A_2E	25069.20	-0.41	-0.37	-0.04		A_2E	21654.22	1.59	1.83	-0.14
	EA_1			-0.33	-0.08		EA_1	21655.12	2.49	3.36	-0.87

Table 2 (continued).

$J_{K_-K_+} - J'_{K_-'K_+'}$	$\tilde{\nu}_n$ $\Gamma\Gamma'$	ν_{exp}	$\Delta\nu_{exp}$	$\Delta\nu_{cal}$	$\Delta\nu_{exp} - \Delta\nu_{cal}$	$J_{K_-K_+} - J'_{K_-'K_+'}$	$\tilde{\nu}_n$ $\Gamma\Gamma'$	ν_{exp}	$\Delta\nu_{exp}$	$\Delta\nu_{cal}$	$\Delta\nu_{exp} - \Delta\nu_{cal}$
$6_{06} - 6_{15}$	1_1 A_1A_2	26723.69				$6_{24} - 7_{17}$	1_1 A_1A_2	32857.32			
	EE	26724.01	0.32	0.37	−0.05		EE	32856.58	−0.74	−0.83	0.09
	A_1E	26724.34	0.65	0.68	−0.03		A_1E	32855.88	−1.44	−1.54	0.10
	EA_2			0.70	−0.05		EA_2			−1.58	0.14
	1_2 A_2A_1	26353.66					1_2 A_2A_1	33339.64			
	EE	26353.95	0.29	0.30	−0.01		EE	33339.00	−0.64	−0.71	0.07
	A_2E	26354.25	0.59	0.55	0.04		A_2E	33338.34	−1.30	−1.26	−0.04
	EA_1			0.57	0.02		EA_1			−1.32	0.02
$7_{07} - 7_{16}$	1_1 A_1A_2	29845.76				$7_{34} - 8_{27}$	1_1 A_1A_2	20217.50			
	EE	29846.11	0.35	0.43	−0.08		EE	20216.73	−0.77		
	A_1E	29846.45	0.69	0.76	−0.07		A_1E	20215.96	−1.54		
	EA_2			0.80	−0.11		EA_2				
	1_2 A_2A_1	29332.25					1_2 A_2A_1	20315.31			
	EE	29332.57	0.32	0.33	−0.01		EE	20314.59	−0.72		
	A_2E	29332.85	0.64	0.61	0.03		A_2E	20313.87	−1.45		
	EA_1			0.64	0.00		EA_1				
$5_{24} - 6_{15}$	1_1 A_1A_2	36700.52				$7_{35} - 8_{26}$	1_1 A_1A_2	24045.41			
	EE	36699.99	−0.53	−0.55	0.02		EE	24044.68	−0.73		
	A_1E	36699.47	−1.05	−1.05	0.00		A_1E	24043.95	−1.47		
	EA_2			−1.08	0.03		EA_2				
	1_2 A_2A_1	36447.68					1_2 A_2A_1	23866.33			
	EE	36447.17	−0.51	−0.52	0.01		EE	23865.64	0.69		
	A_2E	36446.68	−1.01	−0.89	−0.12		A_2E	23864.96	1.37		
	EA_1			−0.94	−0.07		EA_1				

in combination were also necessary to assign the EA_i-components. For the A_iE-components it was necessary to record the spectra with low Stark field (20—200 V/cm) as they have a strong linear contribution to the Stark effect. At higher voltages they are broadened or smeared out, as the basis of the Stark square wave is not ideally zeroed and the Stark field is inhomogeneous.

The multiplets of the $\Delta J = 1$ line $2_{02} - 1_{11}$ were located by MW-MW-DR experiments. To connect the line with the assigned line $2_{02} - 2_{11}$ we kept the signal source fixed to the components of the $2_{02} - 2_{11}$ line and swept the pump. Initial searches were made over 3 GHz with unstabilised pump sources. A sweep over 1.5 GHz is shown in Figure 3. The roughly determined frequencies were refined by stabilised sweeps of the pump source and by measurements with the Stark spectrometer.

The measured spectra are given in Tables 5—7. In Table 8 the A_iA_j- and A_iE-rotational constants are listed.

Analysis of the Torsional Splittings

The analysis is based on the rigid frame-rigid top model. The Hamiltonian is given in Eq. (2):

$$\begin{aligned}\mathcal{H} = {} & AP_a^2 + BP_b^2 + CP_c^2 + F_1\mathcal{P}_1^2 + F_2\mathcal{P}_2^2 \\ & + F'(\mathcal{P}_1\mathcal{P}_2 + \mathcal{P}_2\mathcal{P}_1) + F_1 p_1^2 \\ & + \frac{V_3}{2}(1 - \cos 3\alpha_1) + F_2 p_2^2 \\ & + \frac{V_3}{2}(1 - \cos 3\alpha_2) + F'(p_1p_2 + p_2p_1) \\ & + V_{12}\cos 3\alpha_1 \cos 3\alpha_2 + V'_{12}\sin 3\alpha_1 \sin 3\alpha_2 \\ & - F'(p_1\mathcal{P}_2 + p_2\mathcal{P}_1) - 2F_1 p_1\mathcal{P}_1 - 2F_2 p_2\mathcal{P}_2;\end{aligned} \tag{2}$$

A, B, C rotational constants,

$g = a, b, c$ indices label molecule fixed principal inertia axes,

I_g principal moments of inertia,

I_α moment of inertia of the tops about their symmetry axis,

Table 3. Rotational lines of $(CD_3)_2O$ for the $\tilde{v}_n = 2_1$, 2_2 and 2_3 torsional state [MHz] for $\tilde{v}_n = 2_1$ and 2_3: A_1A_1, EE, A_1E, EA_1, for $\tilde{v}_n = 2_2$: A_2A_2, EE, A_2E, EA_2.

$J_{K_-K_+} - J'_{K_-'K_+'}$	$\tilde{v}_n$ $\Gamma\Gamma'$	ν_{exp}	$\Delta\nu_{exp}$	$\Delta\nu_{cal}$	$\Delta\nu_{exp} - \Delta\nu_{cal}$
$0_{00} - 1_{11}$	2_1 AA	32496.44			
	EE	32491.43	-5.01	-5.16	0.15
	AE	32486.66	-9.78	-9.95	0.17
	EA	32486.16	-10.28	-10.71	0.42
	2_2 AA	32474.24			
	EE	32465.31	-8.94	-8.62	-0.32
	AE	32457.19	-17.06	-16.41	-0.64
	EA	32455.59	-18.65	-18.18	-0.48
	2_3 AA	32512.29			
	EE	32509.32	-2.97	-3.07	0.10
	AE	32506.52	-5.77	-6.07	0.30
	EA	-	-	-6.36	-
$1_{01} - 1_{10}$	2_1 AA	18951.06			
	EE	18946.28	-4.78	-4.79	0.02
	AE	18941.24	-9.82	-9.96	0.14
	EA	18941.76	-9.30	-9.23	-0.08
	2_2 AA	18921.05			
	EE	18912.92	-8.13	-7.77	-0.36
	AE	18904.02	-17.03	-16.44	-0.59
	EA	18905.59	-15.46	-14.79	-0.68
	2_3 AA	18945.12			
	EE	18942.28	-2.85	-2.93	0.08
	AE	18939.43	-5.70	-6.09	0.39
	EA	18939.55	-5.58	-5.80	0.22
$1_{11} - 2_{02}$	2_1 AA	10149.87			
	EE	10154.38	4.51	4.69	-0.18
	AE	10159.10	9.23	9.01	0.22
	EA	-		9.76	-
	2_2 AA	10139.39			
	EE	10147.35	7.96	7.78	0.18
	AE	-	-	14.74	-
	EA	-	-	16.51	-
	2_3 AA	10103.53			
	EE	10106.33	2.80	2.76	0.04
	AE	10108.89	5.36	5.45	-0.09
	EA	-	-	5.74	-
$2_{02} - 2_{11}$	2_1 AA	19645.53			
	EE	19640.57	-4.97	-5.09	0.12
	AE	19635.54	-9.99	-10.30	0.31
	EA	19635.68	-9.85	-10.07	0.22
	2_2 AA	19595.44			
	EE	19586.82	-8.62	-8.36	-0.27
	AE	19578.06	-17.38	-17.04	-0.34
	EA	19578.58	-16.86	-16.54	-0.33
	2_3 AA	19605.38			
	EE	19602.46	-2.92	-3.09	0.17
	AE	19599.54	-5.84	-6.32	0.48
	EA			-6.22	0.38
$3_{03} - 3_{12}$	2_1 AA	20721.48			
	EE	20716.36	-5.13	-5.38	0.25
	AE	20711.23	-10.25	-10.82	0.57
	EA			-10.72	0.47
	2_2 AA	20639.29			
	EE	20630.41	-8.88	-8.90	0.02
	AE	20621.42	-17.87	-17.98	0.11
	EA	20621.61	-17.67	-17.77	0.10
	2_3 AA	20626.77			
	EE	20623.78	-2.99	-3.28	0.29
	AE	20620.77	-6.00	-6.67	0.67
	EA			-6.62	0.62
$2_{12} - 3_{03}$	2_1 AA	24973.62			
	EE	24977.81	4.19	4.26	-0.07
	AE	24981.94	8.31	8.40	-0.09
	EA	24982.08	8.46	8.64	-0.18
	2_2 AA	24936.96			
	EE	24944.36	7.40	6.95	0.45
	AE	24951.46	14.50	13.64	0.86
	EA	24951.99	15.03	14.27	0.76
	2_3 AA	24891.12			
	EE	24893.58	2.46	2.50	-0.04
	AE	24896.04	4.92	5.04	-0.12
	EA			5.14	-0.22
$4_{04} - 4_{13}$	2_1 AA	22219.02			
	EE	22213.65	-5.37	-5.76	0.39
	AE	22208.30	-10.72	-11.54	0.82
	EA			-11.51	0.79
	2_2 AA	22090.70			
	EE	22081.41	-9.28	-9.58	0.30
	AE	22072.13	-18.56	-19.28	0.72
	EA			-19.20	0.64
	2_3 AA	22045.72			
	EE	22042.59	-3.13	-3.54	0.41
	AE	22039.46	-6.26	-7.16	0.90
	EA			-7.14	0.88
$5_{05} - 5_{14}$	2_1 AA	24189.13			
	EE	24183.48	-5.65	-6.24	0.59
	AE	24177.82	-11.31	-12.49	1.18
	EA			-12.50	1.19
	2_2 AA	23998.02			
	EE	23988.23	-9.79	-10.45	0.66
	AE	23978.43	-19.59	-21.00	1.41
	EA			-20.99	1.40
	2_3 AA	23908.70			
	EE	23905.40	-3.30	-3.86	0.56
	AE	23902.12	-6.58	-7.81	1.23
	EA			-7.80	1.22

Table 3 (continued).

$J_{K_-K_+} - J'_{K_-'K_+'}$	$\tilde{\nu}_n$ $\Gamma\Gamma'$	ν_{exp}	$\Delta\nu_{exp}$	$\Delta\nu_{cal}$	$\Delta\nu_{exp} - \Delta\nu_{cal}$	$J_{K_-K_+} - J'_{K_-'K_+'}$	$\tilde{\nu}_n$ $\Gamma\Gamma'$	ν_{exp}	$\Delta\nu_{exp}$	$\Delta\nu_{cal}$	$\Delta\nu_{exp} - \Delta\nu_{cal}$
$4_{23} - 5_{14}$	2_1 AA	20221.96				$5_{23} - 6_{16}$	2_3 AA	21868.51			
	EE	20233.49	11.53	14.60	-3.07		EE	21876.04	7.53	9.20	-1.67
	AE	20243.47	21.51	25.40	-3.89		AE	21883.74	15.22	19.29	-4.07
	EA	20247.05	25.09	32.70	-7.61		EA	21883.22	14.71	17.97	-3.26
	2_2 AA	20093.56				$6_{06} - 6_{15}$	2_1 AA	26690.32			
	EE	20115.00	21.44	24.90	-3.46		EE	26684.29	-6.03	-6.85	0.82
	AE	20131.21	37.65	41.30	-3.65		AE	26678.24	-12.08	-13.69	1.61
	EA	20141.26	47.70	58.00	-10.30		EA			-13.74	1.65
	2_3 AA	19904.61					2_2 AA	26416.94			
	EE	19910.53	5.92	8.25	-2.33		EE	26406.51	-10.43	-11.56	1.13
	AE	19916.58	11.97	15.25	-3.28		AE	26396.08	-20.86	-23.19	2.33
	EA			18.28	-6.31		EA			-23.22	2.36
$5_{23} - 6_{16}$	2_1 AA	21544.57					2_3 AA	26269.39			
	EE	21557.22	12.65	14.87	-2.22		EE	26265.90	-3.48	-4.28	0.80
	AE	21570.55	25.98	31.36	-5.38		AE	26262.42	-6.97	-8.64	1.67
	EA	21569.24	24.67	28.18	-3.51		EA			-8.64	1.67
	2_2 AA	21787.37									
	EE	21808.89	21.52	24.04	-2.52						
	AE	21832.57	45.20	52.03	-6.83						
	EA	21828.31	40.94	44.65	-3.71						

λ_{gi} direction cosine between axis of top i and principal inertia axis g,

P_g g-component of total angular momentum,

p_i total angular momentum of top i along its symmetry-axis.

$$\mathscr{P}_i = \sum_g \lambda_{gi} I_\alpha P_g / I_g, \quad i = 1, 2;$$

$$F = \frac{\hbar}{4\pi} \frac{I_\alpha \left(1 - \sum_g \lambda_{gi}^2 I_\alpha / I_g\right)}{N},$$

$$F' = \frac{\hbar}{4\pi} \frac{I_\alpha{}^2 \sum_g \lambda_{g_1} \lambda_{g_2} / I_g}{N},$$

$$N = I_\alpha{}^2 \left(1 - \sum_g \lambda_{g_1}^2 I_\alpha / I_g\right)\left(1 - \sum_g \lambda_{g_2}^2 I_\alpha / I_g\right) - \left(\sum_g \lambda_{g_1} \lambda_{g_2} I_\alpha{}^2 / I_g\right)^2.$$

Discussions of the model and Hamiltonian may be found in Refs. [2—8], [11], [21].

Computer programs MELITA and MELISA originally written by Trinkaus [11, 22] and modified by Tan [23] were adapted to the Digital PDP 10 and TR 440.

Because of the size of the program overlay technique has to be used. Both programs use van Vleck perturbation for the torsional levels and diagonalisation of the effective rotational matrix. In MELISA denominator correction is included. Details are given in [11, 18].

Trial calculations for $(CH_3)_2O$ showed, that a basis set of uncoupled Mathieu functions for the two internal rotors with $v_{max} = v_1 + v_2 = 8$ * is sufficient [18]. In the worst case the calculated splittings for 2_n-states changed by 2.2% using an extended basis set with $v_{max} = 9$, which is less of than the error of the fitted splittings (see Table 10).

For $(CD_3)_2O$ we observed difficulties in the convergence of the eigenvalues when v_{max} is varied. Limited by the computer size, we used $v_{max} = 9$. Similar observations were made by Durig et al. [13]. This fact implicates that the results for $(CD_3)_2O$ are less reliable.

We investigated the dependence of the splittings on the potential parameters V_3, V_{12}, V'_{12} on the angle $\sphericalangle(b, i)$ between the b- and internal rotation axis and the rotational constants A, B and C. Table 9 characterises this dependence by a quadratic mean of partial derivatives QMPD(X) defined by:

* v_i is the torsional quantum number of the Mathieu function.

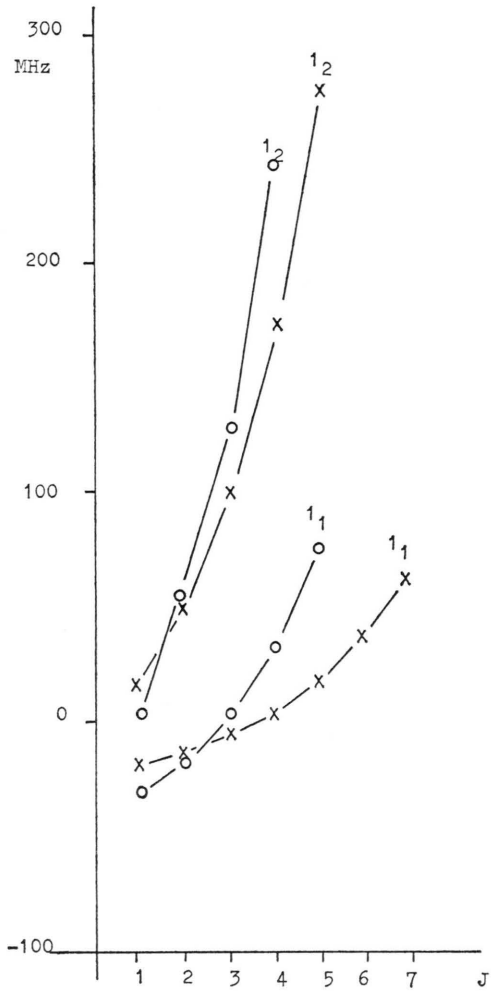

◀ Fig. 1. Plot of the frequency shifts $\nu_{0_1}^{A_1A_1} - \nu_{\tilde{\nu}_n}^{A_iA_j}$ ($\tilde{\nu}_n = 1_1, 1_2$) as function of the rotational quantum number J of the series $J_{0,J} - J_{1,J-1}$. —○— $(CH_3)_2O$; —×— $(CD_3)_2O$.

Table 4. Effective rotational constants and moments of inertia of $(CD_3)_2O$ in torsional axcited states.

$\tilde{\nu}_n$		A, B, C MHz	I_g [c] amu Å²	Δ [b,c] amu Å²
0_1 [a]	A	25696.17 ± 0.11	I_a 19.67340	
	B	7483.79 ± 0.03	I_b 67.55013	
	C	6798.01 ± 0.06	I_c 74.36456	12.85897
1_1 A_1A_2	A	25701.73 ± 0.09	I_a 19.66914	
	B	7466.97 ± 0.03	I_b 67.70229	
	C	6785.67 ± 0.05	I_c 74.49979	12.87164
1_2 A_2A_1	A	25674.80 ± 0.09	I_a 19.68977	
	B	7448.76 ± 0.03	I_b 67.86781	
	C	6793.73 ± 0.05	I_c 74.41141	13.14617
2_1 A_1A_1	A	25723.78 ± 0.08	I_a 19.65228	
	B	7448.79 ± 0.02	I_b 67.86753	
	C	6772.76 ± 0.03	I_c 74.64180	12.87801
2_2 A_2A_2	A	25697.70 ± 0.08	I_a 19.67223	
	B	7433.62 ± 0.02	I_b 68.00603	
	C	6776.71 ± 0.03	I_c 74.59829	13.07997
2_3 A_1A_1	A	25728.74 ± 0.06	I_a 19.64849	
	B	7427.18 ± 0.02	I_b 68.06499	
	C	6783.64 ± 0.02	I_c 74.52209	13.19140
2_1 A_1E	A	25713.98 ± 0.15	I_a 19.65977	
	B	7448.54 ± 0.04	I_b 67.86981	
	C	6772.72 ± 0.05	I_c 74.64224	12.88734
2_2 A_2E	A	25680.67 ± 0.07	I_a 19.68527	
	B	7433.15 ± 0.02	I_b 68.01033	
	C	6776.60 ± 0.02	I_c 74.59950	13.09610
2_3 A_1E	A	25723.00 ± 0.09	I_a 19.65288	
	B	7427.04 ± 0.02	I_b 68.06628	
	C	6783.62 ± 0.03	I_c 74.52231	13.19686

Errors are twice the standard errors.
[a] Lines not split in ground state.
[b] $\Delta = I_a + I_b - I_c$.
[c] Conversion factor 505 531 amu Å² MHz.

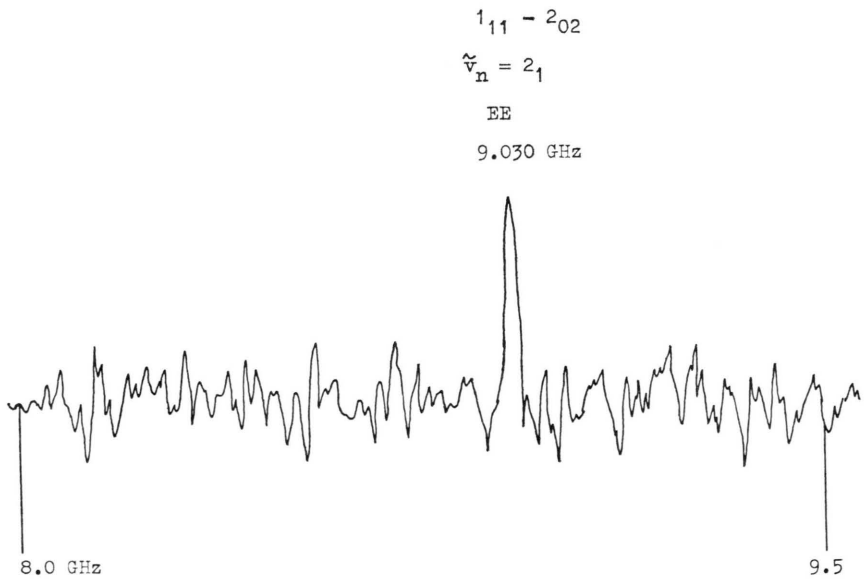

Fig. 3. Recording of a MW-MW-Douple resonance experiment. Signalfrequency 31 584.7 MHz EE component of $2_{02}-2_{11}$, $\tilde{\nu}_n = 2_1$. Pumpfrequency swept unstabilised from 8.5 to 9.5 in 3 min.

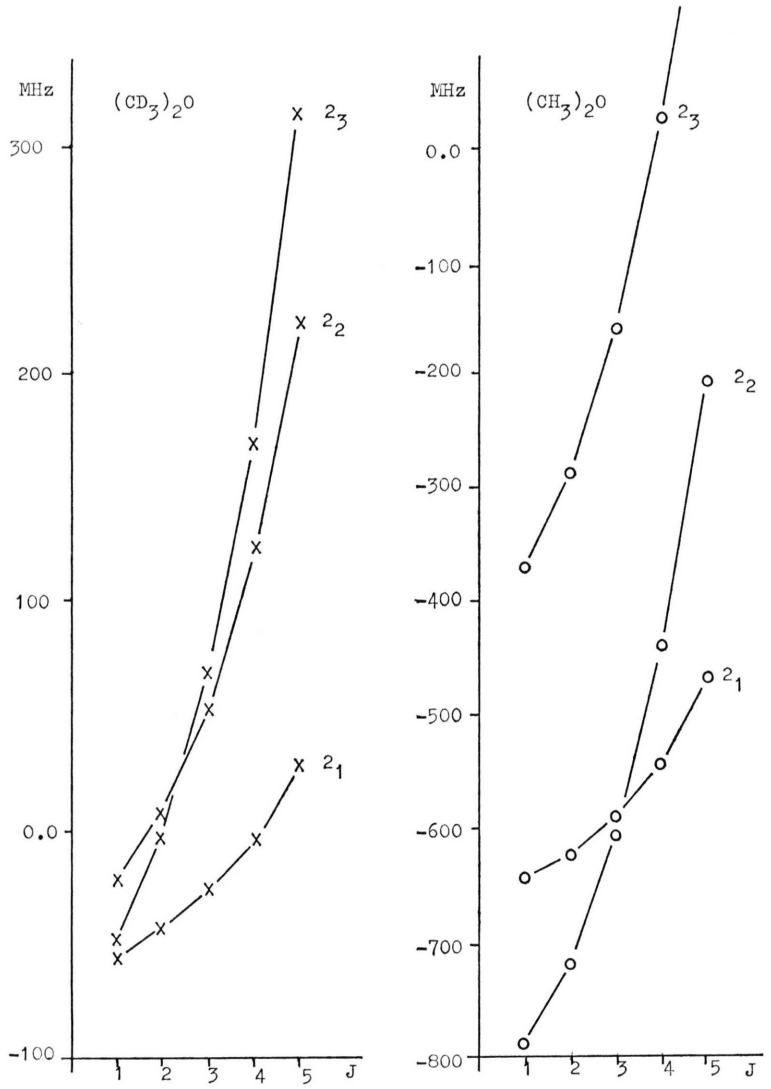

Fig. 2. Plot of the frequency shifts $\nu_{O_1}^{A_1A_1} - \nu_{\tilde{\nu}_n}^{A_iA_j}$ ($\tilde{\nu}_n = 2_1, 2_2, 2_3$) as function of the rotational quantum number J of the series $J_{0,J} - J_{1,J-1}$.

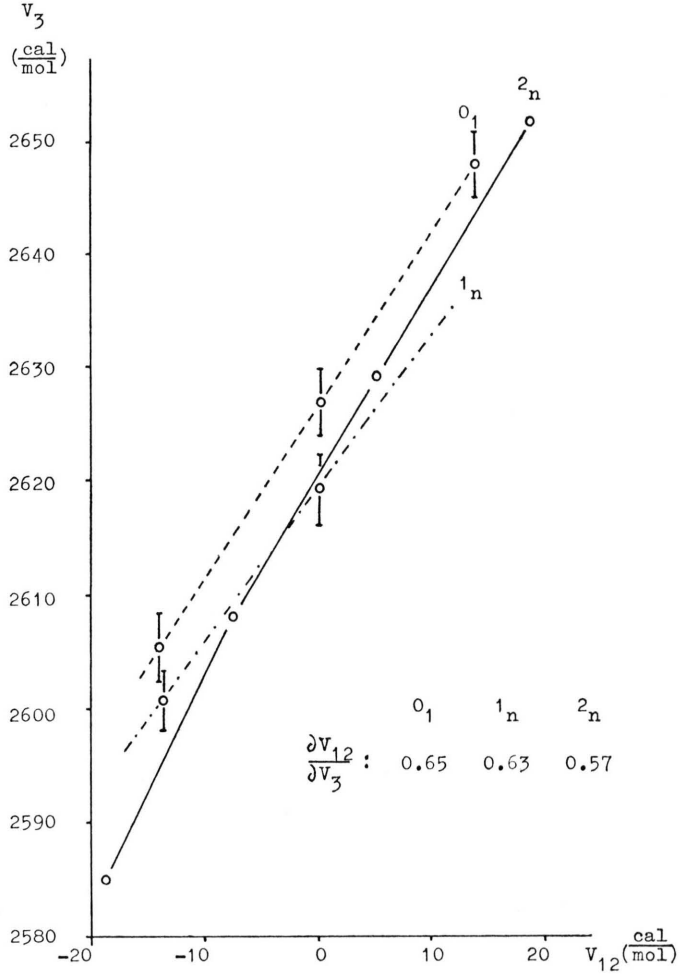

Fig. 4. Correlation of the potential parameters V_3 and V_{12} for the states $\tilde{\nu}_n = 0_1, 1_n, 2_n$ of $(CH_3)_2O$ ($F = 204.20$ GHz, $F' = -40.91$ GHz, $I_\alpha = 3.2084$ amu Å^2).

Table 5. Rotational lines of $(CH_3)_2O$ for the $\tilde{v}_n = 0_1$ torsional state [MHz].

$J_{K-K+} - J_{K-'K+'}$	$\tilde{v}_n$ $\Gamma\Gamma'$	ν_{exp}	$\Delta\nu_{exp}$	$\Delta\nu_{cal}$	$\Delta\nu_{exp} - \Delta\nu_{cal}$
$1_{01} - 1_{10}$	0_1 A_1A_1	29902.29			
	EE	29901.40	-0.89	-0.82	-0.07
	A_1E	29900.48	-1.81	-1.69	-0.12
	EA_1			-1.66	-0.15
$1_{11} - 2_{02}$	0_1 A_1A_1	9118.82[a]			
	EE	9119.67[a]	0.85	0.76	0.09
	A_1E	9120.52[a]	1.70	1.55	0.15
	EA_1			1.55	0.15
$2_{02} - 2_{11}$	0_1 A_1A_1	31107.12			
	EE	31106.20	-0.92	-0.85	-0.07
	A_1E	31105.26	-1.86	-1.74	-0.12
	EA_1			-1.72	-0.14
$2_{21} - 3_{12}$	0_1 A_1A_1	27632.30			
	EE	27629.43	-2.87	-2.88	0.02
	A_1E	27627.56	-4.74	-4.72	-0.02
	EA_1	27625.76	-6.54	-6.87	0.33
$2_{12} - 3_{03}$	0_1 A_1A_1	29091.33			
	EE	29092.12	0.79	0.72	0.07
	A_1E	29092.92	1.59	1.46	0.13
	EA_1			1.45	0.12
$3_{13} - 2_{20}$	0_1 A_1A_1	34684.63[a]			
	EE	34682.59[a]	-2.04	-1.88	-0.16
	A_1E	34679.60[a]	-5.03	-5.00	-0.03
	EA_1	34681.45[a]	-3.18	-2.76	-0.42
$3_{03} - 3_{12}$	0_1 A_1A_1	32979.24			
	EE	32978.29	-0.95	-0.89	-0.07
	A_1E	32977.34	-1.90	-1.81	-0.09
	EA_1			-1.79	-0.11
$4_{04} - 4_{13}$	0_1 A_1A_1	35594.39			
	EE	35593.41	-0.98	-0.94	-0.05
	A_1E	35592.40	-1.99	-1.91	-0.08
	EA_1			-1.90	-0.09
$5_{05} - 5_{14}$	0_1 A_1A_1	39048.33			
	EE	39047.26	-1.07	-1.01	-0.07
	A_1E	39046.26	-2.07	-2.04	-0.03
	EA_1			-2.03	-0.04
$5_{24} - 6_{15}$	0_1 A_1A_1	37533.69			
	EE	37535.80	2.11	2.09	0.02
	A_1E	37537.92	4.23	4.24	-0.01
	EA_1			4.26	-0.03
$6_{25} - 5_{32}$[b]	0_1 A_1A_1	33399.68[a]			
	EE	33397.49[a]	-2.19	-1.70	-0.49
	A_1E	33392.76[a]	-6.92	-8.06	1.14
	EA_1	33397.15[a]	-2.53	-0.75	-1.78

[a] Frequencies measured in this work; the other lines are from Ref. [19, 20].

[b] Not used for torsional analysis second order perturbation theory not sufficient.

$$\mathrm{QMPD}(X) = \sqrt{\frac{1}{n}\sum_{1}^{n}\left(\frac{\partial \Delta\nu_i}{\partial X}\right)^2} \qquad (3)$$

n number of used splittings,

$\Delta\nu_i$ multiplet splitting,

X, V_3, V_{12}, V'_{12}, $\sphericalangle(b,i)$, A, B, C.

It may be observed that there is a noticeable dependence of the 1_n-splittings on V'_{12} and of the 2_n-splittings on V_{12} for both molecules.

In Table 10 we present sets of parameters which were fitted to the torsional fine structure of the rotational lines in the states $\tilde{v}_n$. These sets we consider as the final ones of the analysis. They resulted from many attempts described in more detail in [18]. The rotational constants were chosen from the respective fits to the ground state spectra (see Tables 4 and 8), as their variation was nearly without influence if the 2_n-states of $(CH_3)_2O$ are excepted. The fixed parameters are labelled by super f, $\sphericalangle(b,i) = 58.4°$ results from the r_s-structure [19]. I_α was taken from [19]*. Also V_{12} was fixed to $V_{12} = 0$ after noticing, that there exists still a strong correlation to V_3 also in the 2_n-states. The dependence $V_3 = f(V_{12})$ is given in Figure 4.

It must be noticed that for all $\tilde{v}_n$-states $\partial V_{12}/\partial V_3$ is nearly equal so that even by combining all states no reliable value of V_{12} can be determined.

It was proposed [24] to chose another combination of potential parameters: $V_3 - V_{12}$, V_3 to improve the results. We could not proof it.

The sets of parameters of Table 10 were used to calculate $\Delta\nu_{calc}$ of Tables 2, 3, 5—7. Only for the 2_n-states of $(CH_3)_2O$ we used a sightly modified set. Taking the values for s, V_{12}, V'_{12} as given for the 2_n-states in the last column of Table 10 we fitted in addition the angle $\sphericalangle(b,i)$ to $59.5 \pm 0.6°$. σ_{rel} was reduced from 3.5% to 2.9%.

To compare our analysis with results of other authors [12, 13], we give in Table 11 results, which we gained under the assumptions made by these authors: A, B, C ground state values, $V_{12} = 0$, $\sphericalangle(b,i) = 58.4°$. Although the computational methods of [12, 13] were different from ours the agreement of the results is reasonable. For the $\tilde{v}_n = 2_n$-states of $(CH_3)_2O$ no data could be found in the literature.

* The conversion factor was corrected to 505.531 amu Å² · GHz.

Table 6. Rotational lines of $(CH_3)_2O$ for the $\tilde{v}_n = 1_1$ and 1_2 torsional states [MHz].

$J_{K_-K_1} - J'_{K_-'K_+'}$	$\tilde{v}_n\,\Gamma\Gamma'$	ν_{exp}	$\Delta\nu_{exp}$	$\Delta\nu_{cal}$	$\Delta\nu_{exp} - \Delta\nu_{cal}$	$J_{K_-K_1} - J'_{K_-'K_+'}$	$\tilde{v}_n\,\Gamma\Gamma'$	ν_{exp}	$\Delta\nu_{exp}$	$\Delta\nu_{cal}$	$\Delta\nu_{exp} - \Delta\nu_{cal}$
$1_{01} - 1_{10}$	1_1 A_1A_2	29929.98				$3_{03} - 3_{12}$	1_1 A_1A_2	32973.40			
	EE	29957.06	27.08	27.05	0.04		EE	32999.11	25.71	25.74	−0.03
	A_1E	29977.93	47.98	47.71	0.27		A_1E	33023.84	50.44	50.48	−0.04
	EA_2	29990.26	60.28	60.39	−0.11		EA_2	33025.77	52.37	52.52	−0.15
	1_2 A_2A_1	29900.28					1_2 A_2A_1	32848.29			
	EE	29926.22	25.94	25.85	0.09		EE	32872.88	24.61	24.67	−0.06
	A_2E	29946.15	45.88	45.68	0.19		A_2E	32896.52	48.23	48.36	−0.13
	EA_1	29958.05	57.78	57.59	0.19		EA_1	32898.40	50.11	50.28	−0.17
$2_{02} - 2_{11}$	1_1 A_1A_2	31121.93				$4_{04} - 4_{13}$	1_1 A_1A_2	35558.53			
	EE	31147.43	25.50	25.45	0.05		EE	35585.05	26.53	26.63	−0.10
	A_1E	31170.86	48.93	48.82	0.11		A_1E	35611.02	52.50	52.71	−0.21
	EA_2	31174.94	53.01	53.03	−0.02		EA_2	35612.06	53.54	53.87	−0.33
	1_2 A_2A_1	31055.55					1_2 A_2A_1	35348.40			
	EE	31079.95	24.39	24.38	0.01		EE	35373.75	25.34	25.54	−0.20
	A_2E	31102.35	46.80	46.75	0.05		A_2E	35398.54	50.14	50.52	−0.38
	EA_1	-	-	-	-		EA_1	35399.57	51.17	51.60	−0.43
$1_{11} - 2_{02}$	1_1 A_1A_2	8978.34				$5_{05} - 5_{14}$	1_1 A_1A_2	38971.06			
	EE	8959.12	−19.21	−19.10	−0.11		EE	38998.75	27.69	27.93	−0.24
	A_1E	8933.67	−44.67	−44.67	0.00		A_1E	39026.14	55.08	55.54	−0.46
	EA_2	8946.03	−32.30	−31.90	−0.40		EA_2	39026.73	55.67	56.25	−0.42
	1_2 A_2A_1	8917.19					1_2 A_2A_1	38644.50			
	EE	8898.79	−18.40	−18.40	0.00		EE	38670.95	26.45	26.81	−0.36
	A_2E	8874.39	−42.80	−42.75	−0.05		A_2E	38697.07	52.57	53.26	−0.31
	EA_1	8886.42	−30.77	−30.80	0.03		EA_1	38697.67	53.17	53.91	−0.74
$2_{12} - 3_{03}$	1_1 A_1A_2	28890.84				$4_{23} - 5_{14}$	1_1 A_1A_2	14863.06			
	EE	28870.72	−20.12	−20.23	0.10		EE	14821.70	−41.36	−36.35	−5.01
	A_1E	28848.52	−42.32	−42.67	0.35		A_1E	14741.93	−121.13	−128.51	7.38
	EA_2	28852.70	−38.15	−38.30	0.15		EA_2	14819.25	−43.81	−30.00	−13.81
	1_2 A_2A_1	28773.94					1_2 A_2A_1	14508.03			
	EE	28754.63	−19.31	−19.42	0.12		EE	14468.90	−39.13	−35.22	−3.91
	A_2E	28733.36	−40.59	−40.82	0.23		A_2E	14391.57	−116.46	−122.95	6.49
	EA_1	28737.36	−36.58	−36.76	0.18		EA_1	14465.90	−42.13	−29.15	−12.98

Discussion

It must be stated, that the potential coefficient V_{12} could not be determined in spite of many efforts. But V_3 and V'_{12} are reliable values. It should be mentioned, that as in similar work only the splittings of the multipletts have been used in the analysis.

No decission can be made between the results of two quantum chemical calculations [25, 26] for V_{12} and V'_{12}.

As in similar molecules, there is a difference in the effective potential parameters for the CH_3- and CD_3 isotopes [23, 27, 28].

Further work should include more experimental data. Highly resolved infrared and Raman bands would be of use. They are presently not available. The analysis should perhaps be based on a more general Hamiltonian, as there is an interaction of the $\tilde{v}_n = 2_n$-states to the COC-bending state, which we noticed from the rotational spectrum [18] in the first excited bending state.

For other molecules the situation may be more favourable, as for $(CH_3)_2O$ F' dominates V_{12} and V'_{12} in the influence on the splittings. $(CH_3)_2S$ may be a possible candidate.

Table 7. Rotational lines of $(CH_3)_2O$ for the $\tilde{v}_n = 2_1$, 2_2 and 2_3 torsional states [MHz], for $\tilde{v}_n = 2_1$ and 2_3: A_1A_1, EE, A_1E, EA_1, for $\tilde{v}_n = 2_2$: A_2A_2, EE, A_2E, EA_2.

$J_{K_-K_+} - J_{K_-'K_+'}$	$\tilde{v}_n$ $\Gamma\Gamma'$	ν_{exp}	$\Delta\nu_{exp}$	$\Delta\nu_{cal}$	$\Delta\nu_{exp} - \Delta\nu_{cal}$
$1_{01} - 1_{10}$	2_1 AA	30543.46			
	EE	30653.48	110.02	119.86	-9.84
	AE	29878.13	-665.33	-646.60	-18.73
	EA	- [a]	-	564.70	-
	2_2 AA	30691.47			
	EE	31094.93	403.46	422.84	-19.38
	AE	29634.61	-1056.86	-1060.23	3.37
	EA	-	-	-	-
	2_3 AA	30279.18			
	EE	30276.88	-2.30	-5.77	3.47
	AE	29928.78	-350.40	-338.09	-12.31
	EA	-	-	171.45	-
$2_{02} - 2_{11}$	2_1 AA	31729.03			
	EE	31584.75	-144.28	-134.28	-10.00
	AE	31057.96	-671.07	-655.27	-15.80
	EA	- [a]	-	30.03	-
	2_2 AA	31827.14			
	EE	31787.16	-39.98	-31.31	-8.68
	AE	30770.16	-1056.98	-1066.16	9.17
	EA	32297.64	470.50	503.91	-33.41
	2_3 AA	31403.78			
	EE	31288.53	-115.25	-113.06	-2.19
	AE	31048.96	-354.82	-344.44	-10.38
	EA	-	-	-116.57	-
$3_{03} - 3_{12}$	2_1 AA	33569.01			
	EE	33324.29	-244.72	-236.49	-8.24
	AE	32887.36	-681.65	-670.54	-11.11
	EA	33254.43	-314.58	-293.43	-21.15
	2_2 AA	33586.76			
	EE	33311.17	-275.59	-274.60	-0.99
	AE	32524.62	-1062.14	-1080.93	18.79
	EA	33455.81	-130.95	-112.42	-18.53
	2_3 AA	33146.79			
	EE	32994.13	-152.66	-149.65	-3.01
	AE	32784.80	-361.99	-354.71	-7.28
	EA	32903.63	-243.16	-240.40	-2.76
$4_{04} - 4_{13}$	2_1 AA	36135.87			
	EE	35840.21	-295.66	-290.33	-5.34
	AE	35436.42	-699.45	-694.72	-4.73
	EA	35643.96	-491.91	-475.79	-16.12
	2_2 AA	36036.59			
	EE	35639.35	-397.24	-404.75	7.50
	AE	34959.49	-1077.10	-1110.47	33.36
	EA	35510.90	-525.69	-523.57	-2.12
	2_3 AA	35574.08			
	EE	35401.77	-172.31	-170.43	-1,88
	AE	35201.37	-372.71	-369.71	-3.00
	EA	35265.78	-308.30	-306.21	-2.09
$5_{05} - 5_{14}$	2_1 AA	39521.11			
	EE	39189.63	-331.46	-329.95	-1.51
	AE	38794.23	-726.88	-730.28	3.40
	EA	38914.16	-606.95	-597.78	-9.20
	2_2 AA	39261.07			
	EE	38788.24	-472.83	-492.41	19.58
	AE	38154.80	-1106.27	-1160.99	54.72
	EA	38477.85	-783.22	-802.05	18.83
	2_3 AA	38769.23			
	EE	38582.05	-187.18	-187.63	0.45
	AE	38735.46	-393.77	-390.34	-3.43
	EA	38417.29	-351.94	-353.42	1.48
$1_{11} - 2_{02}$	2_1 AA	8283.53			
	EE	9030.36	746.83	737.46	9.37
	AE	-	-	599.10	-
	EA	-	-	1814.20	-
	2_2 AA	8109.00			
	EE	9544.79	1435.79	1454.12	-18.33
	AE	-	-	979.59	-
	EA	-	-	3318.28	-
	2_3 AA	8383.20			
	EE	-	-	325.48	-
	AE	-	-	313.67	-
	EA	-	-	831.25	-
$2_{12} - 3_{03}$	2_1 AA	28158.87			
	EE	28638.56	479.69	473.32	6.37
	AE	28739.27	580.40	564.48	15.93
	EA	-	-	1265.41	-
	2_2 AA	27958.78			
	EE	28921.73	962.95	979.55	-16.60
	AE	28872.13	913.35	917.16	-3.81
	EA	-	-	2556.25	-
	2_3 AA	28154.74			
	EE	28380.54	225.80	213.66	12.14
	AE	28465.07	310.33	296.60	13.73
	EA	-	-	535.98	-

[a] EA_i-components could not be assigned unambiguously.

Table 8. Effective rotational constants and moments of inertia of $(CH_3)_2O$ in torsional excited states.

$\tilde{v}_n$		A, B, C MHz	I_g[c] amu Å^2	Δ[b,c] amu Å^2
0_1 A_1A_1	A	38788.46[a]	I_a 13.03303	
	B	10056.48[a]	I_b 50.26918	
	C	8886.87[a]	I_c 56.88516	6.417049
1_1 A_1A_2	A	38797.34 ± 0.30	I_a 13.03004	
	B	10024.95 ± 0.05	I_b 50.42728	
	C	8867.34 ± 0.10	I_c 57.01045	6.446882
1_2 A_2A_1	A	38770.43 ± 0.30	I_a 13.03909	
	B	9993.07 ± 0.05	I_b 50.58816	
	C	8870.13 ± 0.10	I_c 56.99249	6.634751
2_1 A_1A_1	A	39394.67 ± 0.44	I_a 12.83247	
	B	10003.35 ± 0.09	I_b 50.53617	
	C	8851.08 ± 0.13	I_c 57.11518	6.253465
2_2 A_2A_2	A	39571.26 ± 0.17	I_a 12.77521	
	B	9984.53 ± 0.04	I_b 50.63143	
	C	8879.56 ± 0.05	I_c 56.93199	6.474645
2_3 A_1A_1	A	39131.42 ± 0.32	I_a 12.91880	
	B	9946.58 ± 0.06	I_b 50.82461	
	C	8852.25 ± 0.09	I_c 57.10763	6.63578
1_1 A_1E	A	38845.39 ± 0.23	I_a 13.01393	
	B	10026.04 ± 0.04	I_b 50.42180	
	C	8867.44 ± 0.08	I_c 57.00980	6.425929
1_2 A_2E	A	38816.41 ± 0.23	I_a 13.02364	
	B	9994.10 ± 0.04	I_b 50.58294	
	C	8870.23 ± 0.08	I_c 56.99187	6.614709
2_1 A_1E	A	38717.34 ± 3.29	I_a 13.05360	
	B	9988.42 ± 0.70	I_b 50.61171	
	C	8845.67 ± 0.99	I_c 57.15011	6.515200
2_2 A_2E	A	38508.39 ± 7.76	I_a 13.12781	
	B	9960.89 ± 1.65	I_b 50.75159	
	C	8865.29 ± 2.34	I_c 57.02363	6.855770
2_3 A_1E	A	38781.98 ± 2.58	I_a 13.03520	
	B	9939.18 ± 0.55	I_b 50.86245	
	C	8851.03 ± 0.78	I_c 57.11550	6.782150

Errors are twice the standard errors.
[a] See Ref. [19], [b] and [c] see Table 4.

Table 9. Quadratic mean partial derivatives for the torsional states of $(CH_3)_2O$ and $(CD_3)_2O$.

x	$(CH_3)_2O$			$(CD_3)_2O$	
	0_1	1_n	2_n	1_n	2_n
V_3	12	98	1100	4	47 kHz/cal mol^{-1}
V_{12}	—	—	1900	—	64 kHz/cal mol^{-1}
V'_{12}	—	40	500	3	20 kHz/cal mol^{-1}
$\sphericalangle(b, i)$	110	280	5500	84	490 kHz/Grad
A	—	—	192	—	— kHz/MHz
B	—	—	202	—	— kHz/MHz
C	—	—	145	—	— kHz/MHz

Acknowledgement

We thank Prof. Dr. H. D. Rudolph and Dr. B. Tan, Ulm, for supplying the revised version of the used programs, Dr. P. Groner, Zürich for test calculations with a program developed at the ETH Zürich and Prof. Dr. D. H. Sutter for helpful comments and discussions.

The work was made possible by funds of the Deutsche Forschungsgemeinschaft and Fonds der Chemie.

The calculations were performed at the computer centers of the Universities of Kiel and Hamburg.

Table 10. Results of the analysis of the torsional fine structure.

	$(CD_3)_2O$		$(CH_3)_2O$		
	1_n	2_n	0_1	1_n	2_n
s	103.39 ± 0.80	103.14 ± 0.19	60.32 ± 0.16	59.96 ± 0.02	59.76 ± 0.9
V_3 [cal/mole]	2584 ± 20	2572 ± 6	2630 ± 7	2663 ± 2	2618 ± 4
V_{12} [cal/mole]	0.0[f]	0.0[f]	0.0[f]	0.0[f]	0.0[f]
V'_{12} [cal/mole]	21 ± 50	29 ± 12	0.0[f]	13 ± 2	18 ± 8
$\sphericalangle(b, i)$	58.6 ± 2.0	58.4[f]	57.7 ± 8	60.6 ± 0.2	58.4[f]
F [GHz]	116.51	116.25	203.24	207.02	204.20
F' [GHz]	−33.60	−33.28	−39.7	−44.44	−40.91
I_α [amu Å^2][a]	6.4294[f]	6.4294[f]	3.2084[f]	3.2084[f]	3.2084[f]
σ [MHz]	0.07	0.40	0.14	0.19	16.46
σ [rel%]	10.1	4.5	6.3	0.5	3.5
	1	1	1	1	1
Corr. C	−0.6 1	−0.6 1	−0.6 1	−0.4 1	−0.2 1
	0.3−0.9 1			−0.6−0.2 1	

Errors are twice the standard errors. σ mean square deviation of the splittings, $\sigma_{rel} = \left(\sigma \Big/ \frac{1}{n} \sum_1^n \Delta\nu_i\right) \cdot 100$.
$\Delta\nu_i$ multiplett splitting, n number of lines. Corr. C Elements of the correlation matrix.
[a] Taken from [19] conversion factor changed to 505.531 amu Å^2 GHz. [f] parameter fixed.

Table 11. Comparison of the torsional parameters.

	$(CD_3)_2O$				$(CH_3)_2O$		
	1_n[a]	1_n [13]	$1_n + 2_n$ [12]	2_n[a]	1_n[a]	1_n [13]	$0_1 + 1_n$ [12]
s	103.58 ± 0.05	— *b*	— *b*	103.14 ± 0.19	59.79 ± 0.06	— *b*	— *b*
V_3 [cal/mole]	2583 ± 4	2564.7	2580 ± 64	2572 ± 6	2619 ± 3	2599 ± 1.4	2605 ± 14
V_{12} [cal/mole]	0.0[f]	0.0[f]	17 ± 17	29 ± 12	14 ± 7	14.5 ± 4.6	17 ± 17
$\sphericalangle$ (b, i)	58.4	58.4[f]	— *b*	58.4[f]	58.4[f]	58.4[f]	— *b*
F [GHz]	116.25	116.04[c]	— *b*	116.25	204.20	203.36	— *b*
F' [GHz]	−33.28	−33.37[c]	— *b*	−33.28	−40.91	−41.09	— *b*
I_α [amu Å^2]	6.4294[f]	6.4511[f]	— *b*	6.4294[f]	3.2084[f]	3.2282[f]	— *b*

Assumed $V_{12} = 0$, rotational constants from ground state, [a] this work, [b] no data given, [c] mean value of Table 7 of [13], [f] parameter fixed.

[1] P. H. Kasai and R. J. Myers, J. Chem. Phys. **30**, 1096 (1959).
[2] D. R. Herschbach, J. Chem. Phys. **31**, 91 (1959).
[3] J. D. Swalen and C. C. Costain, J. Chem. Phys. **31**, 1562 (1959).
[4] L. Pierce, J. Chem. Phys. **34**, 498 (1961).
[5] H. Dreizler and H. D. Rudolph, Z. Naturforsch. **17a**, 712 (1962).
[6] R. J. Myers and E. B. Wilson jr., J. Chem. Phys. **33**, 186 (1960).
[7] H. Dreizler, Z. Naturforsch. **16a**, 1354 (1960).
[8] H. Dreizler, Fortschr. Chem. Forsch. **10**, 59 (1968).
[9] J. R. Durig and Y. S. Li, J. Mol. Structure **13**, 459 (1972) (CH_3OCD_3).
[10] E. Hirota, C. Matsumura, and Y. Morino, Bull. Chem. Soc. Japan **40**, 1124 (1967).
[11] A. Trinkaus, H. Dreizler, and H. D. Rudolph, Z. Naturforsch. **28a**, 750 (1973).
[12] M. Hayashi and M. Imachi, Chemistry Letters 1975, Chem. Soc. Japan **1975**, 1249.
[13] J. R. Durig, Y. S. Li, and P. Groner, J. Mol. Spectrosc. **62**, 159 (1976).
[14] H. Lutz and H. Dreizler, Z. Naturforsch. **31a**, 1026 (1976).
[15] H. D. Rudolph, Z. Angew. Phys. **13**, 401 (1961).
[16] U. Andresen and H. Dreizler, Z. Angew. Phys. **30**, 407 (1970).
[17] G. K. Pandey and H. Dreizler, Z. Naturforsch. **31a**, 357 (1976).
[18] H. Lutz, Ph. D. Thesis, Kiel 1978.
[19] U. Blukis, P. Kasai, and R. J. Myers, J. Chem. Phys. **38**, 2753 (1963).
[20] F. J. Lovas, private communication, to be published.
[21] M. Hayashi, private communication 1964.
[22] A. Trinkaus, Ph. D. Thesis, Freiburg 1969.
[23] B. Tan, Diplom Thesis, Freiburg 1972.
[24] P. Groner and J. R. Durig, J. Chem. Phys. **66**, 1856 (1977).
[25] J. R. Hoyland, J. Chem. Phys. **49**, 1908 (1968).
[26] D. Cremer, J. S. Blinkley, J. A. Pople, and W. J. Hehre, J. Amer. Chem. Soc. **96**, 1908 (1968).
[27] J. F. Beecher, J. Mol. Spectrosc. **4**, 414 (1966).
[28] G. K. Pandey, H. Lutz, and H. Dreizler, Z. Naturforsch. **31a**, 1413 (1976).